Wavefront invasion for a chemotaxis model of Multiple Sclerosis

R. Barresi, E. Bilotta, F. Gargano, M. C. Lombardo, P. Pantano & M. Sammartino

Ricerche di Matematica

ISSN 0035-5038

Ricerche mat.
DOI 10.1007/s11587-016-0265-0

Springer

Ricerche mat.
DOI 10.1007/s11587-016-0265-0

Wavefront invasion for a chemotaxis model of Multiple Sclerosis

R. Barresi[1] · E. Bilotta[3] · F. Gargano[2] · M. C. Lombardo[1] · P. Pantano[3] · M. Sammartino[1]

Received: 2 February 2016 / Revised: 11 March 2016

Abstract In this work we study wavefront propagation for a chemotaxis reaction-diffusion system describing the demyelination in Multiple Sclerosis. Through a weakly non linear analysis, we obtain the Ginzburg–Landau equation governing the evolution of the amplitude of the pattern. We validate the analytical findings through numerical simulations. We show the existence of traveling wavefronts connecting two different steady solutions of the equations. The proposed model reproduces the progression of the disease as a wave: for values of the chemotactic parameter below threshold, the wave leaves behind a homogeneous plaque of apoptotic oligodendrocytes. For values of the chemotactic coefficient above threshold, the model reproduces the formation of propagating concentric rings of demyelinated zones, typical of Baló's sclerosis.

✉ R. Barresi
rachelebarresi85@hotmail.com; rachele.barresi@unipa.it

E. Bilotta
eleonora.bilotta@unical.it

F. Gargano
francesco.gargano@unipa.it

M. C. Lombardo
mariacarmela.lombardo@unipa.it

P. Pantano
pietro.pantano@unical.it

M. Sammartino
marcomarialuigi.sammartino@unipa.it

1 Department of Mathematics, University of Palermo, Via Archirafi 34, 90123 Palermo, Italy

2 Department of Energy, Engineering of the Information and Mathematical Models, University of Palermo, Viale delle Scienze Ed.9, 90128 Palermo, Italy

3 Department of Physics, University of Calabria, Via Pietro Bucci, 87036 Rende (CS), Italy

Published online: 31 March 2016

Keywords Chemotaxis · Ginzburg–Landau equation · Multiple Sclerosis

Mathematics Subject Classification 35C07 · 92C17 · 35K57

1 Introduction

Multiple Sclerosis (MS) is an autoimmune debilitating pathology of the central nervous system. In the early stages it is characterized by inflammation and demyelination, with the appearance of focal areas of myelin loss in the white matter of the brain, called plaques or lesions [16]. The pathological hallmark of the initial stages, also common to the so-called type-III pattern of the disease [2,18], mainly consists of an inflammatory state which induces activated macrophages to respond to a chemical stimulus produced by pro-inflammatory mediators, such as cytokines. The whole process results in tissue damage through the destruction of the oligodendrocytes, of the myelin sheath around nerves and of the axons.

Although the immunological mechanisms involved are very complex, some mathematical models, that are able to reproduce the essential features of the disease, have been recently proposed [3,15].

In the present work we shall investigate the dynamics of the following non-dimensional PDE system, describing the interaction between the density of activated macrophages $m = m(t, x)$, the concentration of the cytokine $c = c(t, x)$ and the density of the destroyed oligodendrocytes $d = d(t, x)$:

$$\begin{cases} \frac{\partial m}{\partial t} = \Delta m + \Gamma m\,(1-m) - \nabla \cdot (\chi h(m) \nabla c)\,, & \text{with} \quad h(m) = \frac{m}{1+m}, \\ \frac{\partial c}{\partial t} = \frac{1}{\tau}\left[\epsilon \Delta c + \Gamma(\delta d - c + \beta m)\right], \\ \frac{\partial d}{\partial t} = r \Gamma f(m, d), \qquad \text{with} \quad f(m, d) = \frac{m^2}{1+m}(1-d). \end{cases} \tag{1}$$

We shall solve the above system for $(t, x) \in \mathbb{R}^+ \times \Omega$, where $\Omega = [0, L]$, imposing initial condition and no-flux boundary conditions.

In the above system, the motion of the macrophages is described by two terms: undirected random diffusion and a chemotactic-driven migration term, which accounts for the finite volume of the cells. We therefore adopt a cell-kinetics version of the Keller-Segel model [14] whose density-dependent sensitivity function displays saturation at high cells densities to prevent the blow-up of the solution. The nonnegative parameter χ measures the maximal chemotactic rate. The local dynamics of the macrophages is modeled by an activation front with logistic growth and saturation. The evolution of the cytokine is ruled by a linear diffusion term, whose diffusivity coefficient is ϵ, plus a linear kinetic term, which describes the interaction between species: the nonnegative parameters δ and β are the production rates of cytokine by destroyed oligodendrocytes and macrophages, respectively. The positive constant τ allows for the modeling of the chemoattractant evolution on a different time scale compared to the other two species. The oligodendrocytes are considered fixed in their spatial positions and their dynamics is described by the damaging function $f(m, d)$, that is positive, increasing with respect to $m(x, t)$ and bounded for high values of the macrophages

density. The positive parameter r gives a measure of the destructive strength of the macrophages on the oligodendrocytes. Finally, the non-dimensional parameter Γ is introduced, which governs the spatial and the temporal scales. More details about the derivation of the system (1) and the numerical estimate of the parameters are presented in [3], where an analytical and numerical exploration of the model is also presented.

The mathematical properties of the Keller-Segel system and its numerous variations have been extensively studied, see for example [8,12,13,28] and references therein. Moreover the Keller-Segel chemotaxis model has been proposed to describe aggregation and self organization processes in several biological phenomena. In particular, chemotaxis and motility of macrophages are assumed in some spatially distributed mathematical models of inflammation [7,17,21,22,26].

In this work we first focus on the investigation of the conditions which yield the appearance of stationary non constant solutions for the chemotaxis reaction-diffusion model (1). As the disease-free equilibrium is always unstable, the proposed model prescribes two scenarios. When the chemoattraction is weak (in a sense to be specified after the Turing stability analysis), the activated macrophages do not aggregate and the solutions of the system converge towards the uniform steady state, which corresponds to the formation of a spatially homogeneous plaque [6]. When the chemoattraction is strong, we prove the appearance of periodically spatially distributed clusters of cells. The numerical simulations performed close to the threshold show that, starting form a small perturbation of the disease-free equilibrium, the system evolves towards the formation of a spatially periodic pattern for the macrophages and cytokines. The dynamics of the destroyed oligodendrocytes follows the evolution of the macrophages, forming zones of aggregation which, on a time scale ruled by the system parameters, subsequently evolve towards a spatially uniformly degraded state. This process reproduces the formation of expanding concentric layers of demyelinated white matter, typical of Baló Sclerosis, a very aggressive variant of MS but also frequently seen in the early stages of the pattern III MS lesions [1].

The second goal of the present paper is to study the process of progression of the disease in the form of a wave. We show that, if the chemotactic coefficient is above the critical value, the pattern evolves as a traveling wavefront invading the whole domain. Conversely, when the chemotaxis is weak, a wavefront connecting the disease-free equilibrium to the stable equilibrium corresponding to a homogeneous plaque is found. The issue of existence of traveling wave solutions for reaction-diffusion models has been addressed in many papers, which show that a small perturbation near a homogeneous steady state may lead to a wavefront invasion with the consequent pattern formation [4,9,11,27].

The paper is organized as follows: in Sect. 2 we briefly review some results of the Turing stability analysis obtained in [3]. Section 3 is devoted to derive the Ginzburg-Landau equation governing the amplitude of the pattern, the shape and the speed of the traveling wave. Section 4 provides the numerical simulations, some comparisons with the theoretical results of Sect. 3 and the conclusions.

2 Turing instability analysis

In this Section we briefly outline the results of the Turing stability analysis which describes the mechanism of pattern formation for the system (1).

The two uniform steady states of the system are the disease-free equilibrium $P_0 = (0, 0, 0)$ and the non trivial point $P^* = (m^*, c^*, d^*) = (1, \beta + \delta, 1)$.

The equilibrium P_0 is unstable while P^* is a stable attractive node for the kinetics for all non negative values of the parameters.

The following Turing analysis is aimed to characterize the spacing between cells and the critical value of the chemotactic coefficient above which the pattern may form. This is intended to describe the asymptotic behavior of the solutions of system (1), which corresponds to the case when the macrophage populations is mostly activated and well-delimited zones of destroyed oligodendrocytes are formed.

Linearization around P^* gives:

$$\dot{\mathbf{w}} = \mathcal{L}^{\chi}\mathbf{w} = \Gamma J\mathbf{w} + D^{\chi}\Delta\mathbf{w}, \qquad \text{where } \mathbf{w} = \begin{pmatrix} m - m^* \\ c - c^* \\ d - d^* \end{pmatrix}, \tag{2}$$

$$J = \begin{pmatrix} -1 & 0 & 0 \\ \frac{\beta}{\tau} & -\frac{1}{\tau} & \frac{1}{\tau} \\ 0 & 0 & -\frac{r}{2} \end{pmatrix}, \qquad D^{\chi} = \begin{pmatrix} 1 & -\frac{\chi}{2} & 0 \\ 0 & \frac{\epsilon}{\tau} & 0 \\ 0 & 0 & 0 \end{pmatrix}. \tag{3}$$

The computation of the linear stability analysis can be found in full length in [3]. Here, for brevity, we only report the critical values of the chemotaxis coefficient and of the wavenumber of the resulting pattern, namely:

$$\chi_c = \frac{2(\sqrt{\epsilon} + 1)^2}{\beta}, \qquad k_c^2 = \frac{\Gamma}{\sqrt{\epsilon}}. \tag{4}$$

For $\chi > \chi_c$ the system admits a range $[{k_1}^2, {k_2}^2]$ of unstable wavenumbers. These modes are proportional to Γ, thus for the pattern formation to arise, Γ must be big enough so that at least one of the modes admitted by the boundary conditions lays within the interval $[{k_1}^2, {k_2}^2]$.

We present this result in the following

Theorem 1 *For all non negative values of the parameters $\beta, \delta, \epsilon, r, \tau$, and Γ the equilibrium $P^* = (m^*, c^*, d^*)$ is stable for the kinetics of model (1). Then, if $\chi > \chi_c$, with χ_c given by (4), P^* is an unstable equilibrium for the reaction-diffusion system (1) and spatial patterns may occur close to P^*.*

3 Traveling wavefront equations

In this section we perform a weakly non linear analysis close to the uniform steady state $P^* = (1, \beta + \delta, 1)$ to derive the Ginzburg–Landau amplitude equation for the spatio-temporal pattern for the system (1). In fact, the aim here is to investigate the

process of pattern invasion as a traveling wavefront when the domain is large and to find the form and the amplitude of the resulting wave.

We first assume that the conditions for the Turing instability derived above are satisfied. Following the approach based on the multiple scales method adopted by [5,9,10], we set a small control parameter $\eta^2 = (\chi - \chi_c)/\chi_c$, which gives the dimensionless distance from the bifurcation value of χ. Upon translation of the equilibrium P^* to the origin, the system (1) can be written as:

$$\frac{\partial \mathbf{w}}{\partial t} = \mathcal{L}^{\chi}\mathbf{w} + \mathcal{N}\mathbf{w}, \tag{5}$$

where $\mathbf{w}$ and $\mathcal{L}^{\chi}$ are defined in (2) and $\mathcal{N}$ is a nonlinear operator containing higher order powers in $\mathbf{w}$.

We then expand $\mathbf{w}$, the time derivative $\partial/\partial t$ and the bifurcation parameter χ as follows:

$$\mathbf{w} = \eta\mathbf{w}_1 + \eta^2\mathbf{w}_2 + \eta^3\mathbf{w}_3 + O(\eta^4), \tag{6}$$

$$\chi = \chi_c + \eta\chi_1 + \eta^2\chi_2 + \eta^3\chi_3 + O(\eta^4), \tag{7}$$

$$\frac{\partial}{\partial t} = \eta\frac{\partial}{\partial T_1} + \eta^2\frac{\partial}{\partial T_2} + \eta^3\frac{\partial}{\partial T_3} + O(\eta^4), \tag{8}$$

where $\mathbf{w_i} = (w_i^{(1)}, w_i^{(2)}, w_i^{(3)})^T$.

To describe the phenomenon of wavefront invasion, we need to take into account the slow modulation in space of the pattern amplitude. Therefore, we separate the fast (x) and slow (X) dependencies, so that the spatial derivative and the diffusion operator write as follows:

$$\partial_x \to \partial_x + \eta\partial_X, \quad \partial_{xx} \to \partial_{xx} + 2\eta\partial_{xX} + \eta^2\partial_{XX}. \tag{9}$$

Here, the leading term of the nonlinear expansion of the solution is the product of the basic pattern, which is the solution of the linearized system (2), and a slowly varying amplitude A, depending on both time and the slow spatial variable X. Thus, by substituting the above expansions (9) and (6)–(8) into (2) and collecting the terms at each order of η, we obtain the following systems:

$$O(\eta): \quad \mathcal{L}_x^{\chi_c}\mathbf{w_1} = \mathbf{0}, \tag{10}$$

$$O(\eta^2): \quad \mathcal{L}_x^{\chi_c}\mathbf{w_2} = \mathbf{F}, \tag{11}$$

$$O(\eta^3): \quad \mathcal{L}_x^{\chi_c}\mathbf{w_3} = \mathbf{G}, \tag{12}$$

with $\mathcal{L}_x^{\chi_c} = \Gamma J + D^{\chi_c}\partial_{xx}$. The expressions for $\mathbf{F}$ and $\mathbf{G}$ are too cumbersome and they are not reported here.

From Eq. (10) and taking into account the Neumann boundary conditions, one gets a solution of the form:

$$\mathbf{w_1} = \rho A(X, T_1, T_2, \ldots)\cos(k_c x), \quad \text{with } \rho \in Ker(\Gamma J - k_c^2 D^{\chi_c}), \tag{13}$$

where $A(X, T_1, T_2, \ldots)$ is the amplitude of the pattern (still arbitrary at this level) and ρ is normalized as follows:

$$\rho = \left(M, 1, N\right)^T = \left(\frac{\Gamma+\epsilon k_c^2}{\Gamma\beta}, 1, 0\right)^T.$$

The solvability condition for the Eq. (11) is given by $\langle \mathbf{F}, \psi \cos(k_c x)\rangle = 0$, with

$$\psi = \left(\bar{M}, 1, \bar{N}\right)^T = \left(\frac{\Gamma\beta}{\tau(\Gamma+k_c^2)}, 1, \frac{2\delta}{\tau r}\right)^T \in Ker(\mathcal{L}^*),$$

where we have denoted by $\mathcal{L}^*$ the adjoint of $\mathcal{L}_x^{\chi_c}$ and by $\langle\cdot,\cdot\rangle$ the scalar product in $L^2(0, 2\pi/k_c)$.

Requiring $T_1 = 0$ and $\chi_1 = 0$ to avoid the occurrence of secular terms, the solution to the second-order system (11) is given by:

$$\mathbf{w_2} = A^2\mathbf{w_{20}} + A^2\mathbf{w_{22}}\cos(2k_c x) + \frac{\partial A}{\partial X}\mathbf{w_{21}}\sin(k_c x), \tag{14}$$

where the vectors $\mathbf{w_{2i}} = (w_{2i}^{(1)}, w_{2i}^{(2)}, w_{2i}^{(3)})^T$ for $i = 0, 1, 2$ are the solutions of the following linear systems:

$$\begin{cases} \Gamma J\mathbf{w_{20}} = \left(\frac{\Gamma M^2}{2}, 0, 0\right)^T, \\ (\Gamma J - k_c^2 D^{\chi_c})\mathbf{w_{21}} = 2k_c D^{\chi_c}\rho, \\ (\Gamma J - 4k_c^2 D^{\chi_c})\mathbf{w_{22}} = \left(\frac{\Gamma M^2}{2} - M\chi_c h'(m^*)k_c^2, 0, 0\right)^T. \end{cases} \tag{15}$$

Finally, substituting the expressions of $\mathbf{w_2}$ and $\mathbf{w_1}$ into (12), and imposing the solvability condition at the third order, we get the following Ginzburg-Landau equation for the amplitude $A(X, T_2)$:

$$\frac{\partial A}{\partial T_2} = \nu\frac{\partial^2 A}{\partial X^2} + \sigma A - LA^3, \tag{16}$$

where:

$$\nu = \frac{\langle 2k_c D^{\chi_c}\mathbf{w_{21}} + D^{\chi_c}\rho, \psi\rangle}{\langle\rho, \psi\rangle}, \quad \sigma = \frac{\langle G_1^{(1)}, \psi\rangle}{\langle\rho, \psi\rangle}, \quad L = \frac{\langle G_1^{(3)}, \psi\rangle}{\langle\rho, \psi\rangle}, \tag{17}$$

and

$$G_1^{(1)} = \begin{pmatrix} \chi_2 h(m^*)k_c^2 \\ 0 \\ 0 \end{pmatrix}, \quad G_1^{(3)} = \begin{pmatrix} 2M\Gamma\left(w_{20}^{(1)} + \frac{w_{22}^{(1)}}{2}\right) - \chi_c k_c^2 h'(m^*)(Mw_{22}^{(2)} + w_{20}^{(1)}) \\ +\frac{\chi_c}{2}h'(m^*)k_c^2 w_{22}^{(1)} - \frac{\chi_c}{8}h''(m^*)k_c^2 M^2 \\ 0 \\ 0 \end{pmatrix}.$$

Theorem 2 *Assume that:*

1. *The parameter Γ is sufficiently large (or, equivalently, the spatial domain is large);*
2. *The control parameter $\eta^2 = (\chi - \chi_c)/\chi_c$ is small;*
3. *The Landau coefficient L in (17) is greater than zero.*

Then the emerging solution of the reaction-diffusion system (1) is given by:

$$\begin{pmatrix} m \\ c \\ d \end{pmatrix} = \begin{pmatrix} m^* \\ c^* \\ d^* \end{pmatrix} + \eta \rho A(X, T_2) \cos(k_c x) + O(\eta^2), \tag{18}$$

where $\rho \in \mathrm{Ker}(\Gamma J - k_c^2 D^{\chi_c})$ and $A(X, T_2)$ is the exact solution of the GL equation (16) in $\mathbb{R}$:

$$A(X, T_2) = \frac{1}{2}\sqrt{\frac{\sigma}{L}}\left(1 - \tanh\left(\sqrt{\frac{\sigma}{\nu}}\frac{z - z_0}{2\sqrt{2}}\right)\right), \quad z = X - cT_2, \tag{19}$$

with $c = 3\sqrt{\frac{\sigma\nu}{2}}$, and σ, L and ν given by (17).

In the subcritical case, i.e. when the coefficient L is negative, the third order Ginzburg–Landau equation (16) is not able to capture the amplitude of the pattern. In this case we shall restrict our analysis to a numerical investigation.

4 Numerical simulations and discussion

In this section we present a numerical exploration of system (1). The numerical simulations shown are performed using a finite differences scheme based on the method of the lines. We adopt a 800 points grid for the spatial domain that is able to ensure grid independence of our results. Diffusion terms are approximated by second-order central differences, the taxis term is approximated by a finite difference scheme that conserves the number of macrophages. The time integration is realized using the CVODE stiff integrator included in the XPPAUT computational software package. We set error tolerances of 10^{-10} in CVODE and use a time-step $\Delta t = 10^{-4}$.

We fix the following parameter set $\beta = 1, \delta = 1, r = 1, \tau = 1, \Gamma = 1$ and vary the values of ϵ and χ so as to explore the system behavior under and above the critical threshold χ_c.

We first validate the results obtained by the weakly nonlinear analysis derived in Sect. 2, by reproducing the pattern forming traveling wave solutions for system (1). In the simulation shown in Fig. 1, we choose the parameter values so that they satisfy the hypotheses of Theorem 2, i.e. $\chi > \chi_c, \sigma, L > 0$ and $\eta^2 = 0.033$. We perturb the equilibrium P^* at the left end side of the spatial interval imposing an initial condition of the form $(m_0, c_0, d_0)^T = (m^*, c^*, d^*)^T + \eta A(X, 0)\rho \cos(k_c x)$, where $A(X, T_2)$ is given by (19). After a transient, the solution of the Ginzburg-Landau equation Eq. (16) (shown by the dashed red line) is in good agreement with the amplitude of the

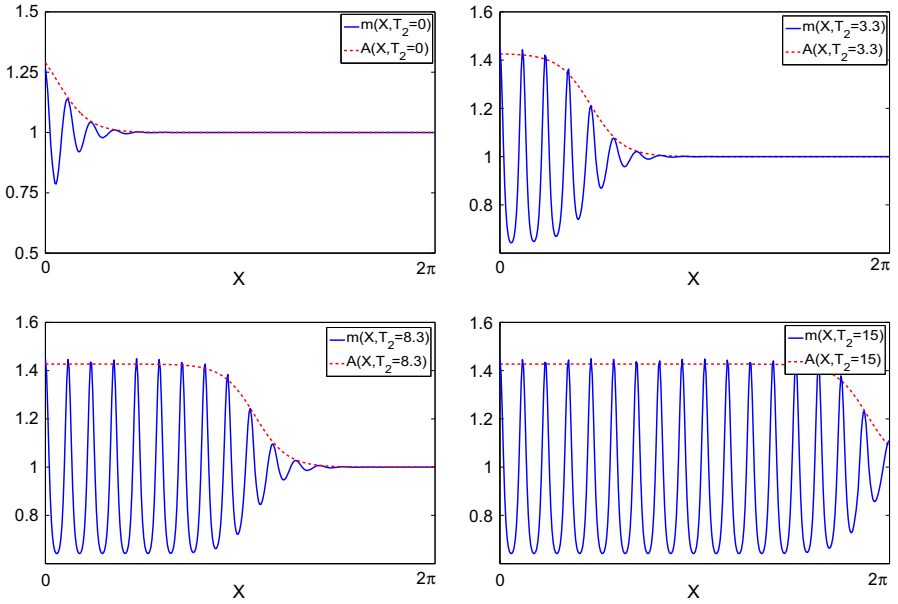

Fig. 1 A localized perturbation of the equilibrium P^* produces a pattern which invades the domain as a modulated traveling wave. The *dashed line* is the exact solution (19) of GL Eq. (16), the *solid line* is the numerical solution of the system (1) with initial condition $(m_0, c_0, d_0)^T = (m^*, c^*, d^*)^T + \eta A(X, 0)\rho \cos(k_c x)$ at the times indicated. The parameter values are: $\beta = 1, \delta = 1, r = 1, \tau = 1, \epsilon = 0.01, \Gamma = 1, \chi = 2.5 > \chi_c = 2.42$ and $\eta^2 = 0.033$

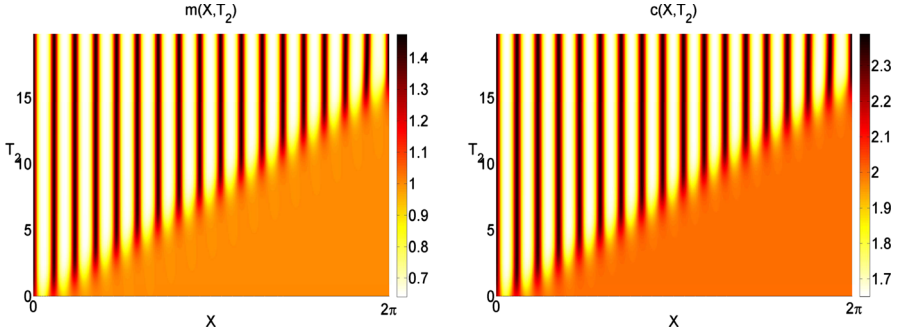

Fig. 2 Pattern invasion as a modulated traveling wave in the supercritical case for the macrophages (*left*) and the cytokine (*right*). In the case of the initial conditions imposed here, the species d remains at the homogeneous equilibrium. The parameter values are chosen as in Fig. 1

numerical solution of the system (1) (solid blue line), and the pattern invades the domain as a traveling wavefront (see Fig. 2).

We now consider the subcritical case, namely the parameters are picked so as to satisfy the conditions of (1) and the coefficient $L < 0$. The simulation in Fig. 3 is performed choosing $\epsilon = 0.8, \chi = 7.24 > \chi_c = 7.17$ and $\eta^2 = 0.009$. We impose as initial condition a random perturbation of the equilibrium $P^* = (1, \delta + \beta, 1)$ at the

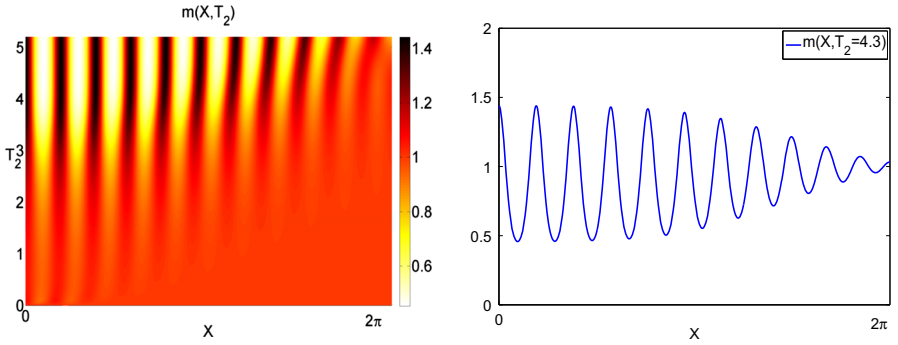

Fig. 3 (*Left*) Pattern invasion as a modulated traveling wave in the subcritical case. (*Right*) Numerical solution of the system (1) with a localized random perturbation of the equilibrium P^* as initial condition at the time indicated. The parameter values are: $\beta = 1, \delta = 1, r = 1, \tau = 1, \epsilon = 0.8, \Gamma = 1, \chi = 7.24 > \chi_c = 7.17$ and $\eta^2 = 0.009$

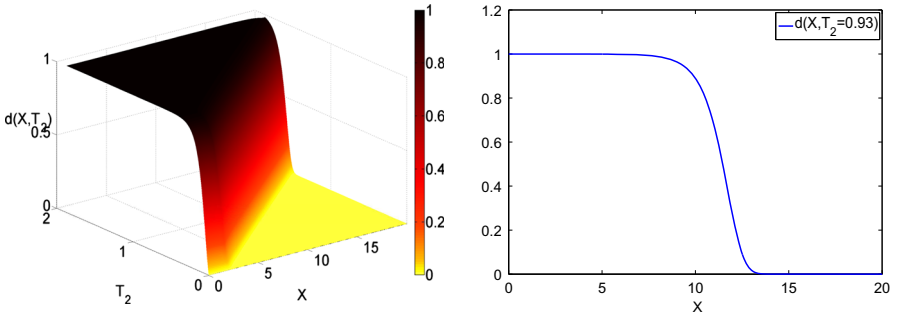

Fig. 4 (*Left*) A traveling wave connects the equilibrium $P^* = (1, b+d, 1)$ to $(0, 0, 0)$. (*Right*) Numerical solution of the system (1) for the oligodendrocytes d species at the time indicated. The initial condition is $(m_0, c_0, d_0) = \eta A(X, 0)\rho$. The parameter values are $\beta = 1, \delta = 1, r = 1, \tau = 1, \epsilon = 0.03, \Gamma = 1, \chi = 2.65 < \chi_c = 2.75$ and $\eta^2 = 0.037$

left end of the spatial domain which produces the formation of a traveling wavefront leaving behind a stationary pattern, whose wavenumber is still predicted by the linear stability analysis. The propagation of the pattern as a traveling wavefront, in both the supercritical and subcritical cases, reproduces the well known phenomenon of the formation of the concentric demyelinated rings [1], typical of Baló's Sclerosis but also found in some early active MS lesions. A similar dynamics was also observed in the 2D numerical simulations of system (1) presented in [3], where the disease progresses as a target pattern, forming spaced concentric demyelinated annuli.

On the other hand, it is also of great biological interest to describe the mechanism of disease invasion, starting from a healthy initial condition. This corresponds to the existence of an orbit connecting the unstable disease-free equilibrium to the stable equilibrium P^*. We therefore choose the chemotactic parameter χ under the threshold χ_c and impose the following small perturbation of the equilibrium P_0 as initial condition: $(m_0, c_0, d_0) = \eta A(X, 0)\rho$. The numerically found traveling wave solution connecting P^* to P_0 is shown in Fig. 4, where the profile of $d(x, t)$ is depicted.

Therefore, when the conditions of Theorem 1 are not satisfied, namely the value of χ is below criticality, the proposed model describes the formation and propagation of a homogeneous plaque which invades the domain. The analytical description of this phenomenon will be the subject of a forthcoming paper. It would be also of interest to rigorously prove that, when the chemotactic coefficient is below the threshold, the disease-free equilibrium is globally asymptotically stable, using the techniques adopted, e.g., in [19,20,23–25].

Since for $\chi > \chi_c$ the equilibrium P^* is unstable, whereas the Turing pattern is stable, one could look for an orbit connecting the free-disease state to the Turing pattern prescribed by the weakly nonlinear expansion. The above described scenario was simulated for two different values of the control parameter χ: close to the bifurcation and well-above the critical threshold. In the former case, shown in Fig. 5, one can see that the species m evolves on two different time scales: on an $O(1)$-scale a wavefront propagates connecting the disease-free equilibrium to the unstable steady state P^* [the

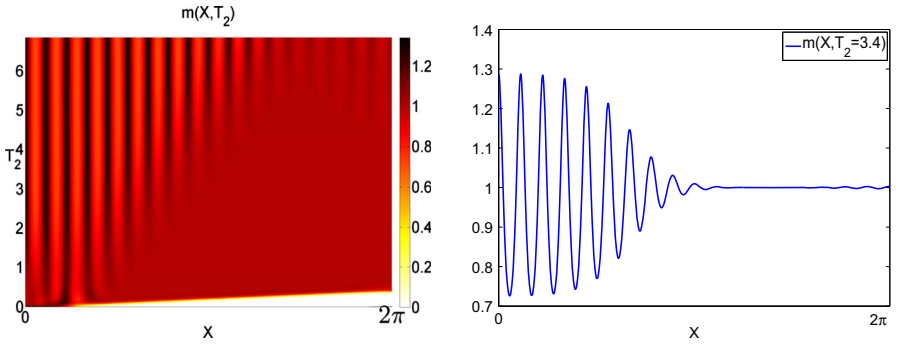

Fig. 5 (*Left*) A traveling wave initially propagates connecting P_0 to P^*. After the wavefront has invaded the domain, a second wave is formed, leaving behind the Turing pattern. (*Right*) Numerical solution of the system (1) for the macrophages m species at the time indicated. The initial condition is a small perturbation of the homogeneous equilibrium P_0 at the left end of the domain. The parameter values are $\beta = 1, \delta = 1, r = 1, \tau = 1, \epsilon = 0.03, \Gamma = 1, \chi = 2.8 > \chi_c = 2.75$ and $\eta^2 = 0.01$

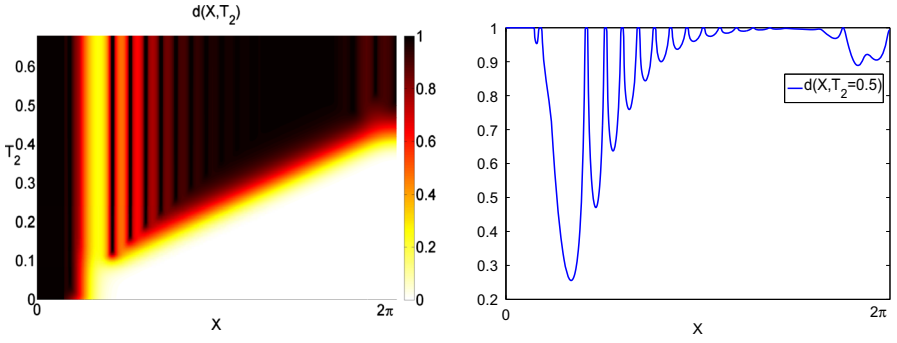

Fig. 6 (*Left*) Fully nonlinear solutions in the form of a traveling wave connecting the pattern to P_0. (*Right*) Numerical solution of the system (1) for the oligodendrocytes d species at the time indicated. The initial condition is a small perturbation of the homogeneous equilibrium P_0 at the left end of the domain. The parameter values are $\beta = 1, \delta = 1, r = 1, \tau = 1, \epsilon = 0.03, \Gamma = 1, \chi = 8.5 \gg \chi_c = 2.75$ and $\eta^2 = 2.09$

dark zone in the bottom of Fig. 5(Left)]. Once the homogeneous plaque has invaded the domain, on an $O(\eta^{-2})$ temporal scale a second wave is initiated, leaving behind the pattern prescribed by the linear stability analysis.

If the chemotaxis coefficient is chosen far away from the bifurcation value, the value of η is big and the two different time scales observed in Fig. 5 can be made of the same order. Then the observed spatio-temporal dynamics of the d describes the onset of well-defined spatially structured plaques around the unstable equilibrium P^*, analogous to the Baló's concentric rings. This is reported in Fig. 6, where $\chi = 8.5 \gg \chi_c = 2.75$. In this fully nonlinear regime, the wavelength and the form of the pattern do not match with the expected solution found through the weakly nonlinear analysis and nonlinear effects in the form of amplitude instabilities and defects appear.

Acknowledgments This work has been partially supported by National Group of Mathematical Physics (GNFM-INDAM) through a "Progetto Giovani" grant.

References

1. Baló, J.: Encephalitis periaxialis concentrica. Archiv. Neurol. Psychiatr. **19**(2), 242–264 (1928)
2. Barnett, M.H., Parratt, J.D.E., Pollard, J.D., Prineas, J.W.: MS: is it one disease? Int. MS J. **16**(2), 57–65 (2009)
3. Barresi, R., Bilotta, E., Gargano, F., Lombardo, M.C., Pantano, P., Sammartino, M.: Demyelination patterns in a mathematical model of Multiple Sclerosis. Submitted (2016)
4. Bilotta, E., Pantano, P.: Emergent patterning phenomena in 2D cellular automata. Artif. Life **11**(3), 339–362 (2005)
5. Bozzini, B., Gambino, G., Lacitignola, D., Lupo, S., Sammartino, M., Sgura, I.: Weakly nonlinear analysis of Turing patterns in a morphochemical model for metal growth. Comp. Math. Appl. **70**(8), 1948–1969 (2015)
6. Cerasa, A., Bilotta, E., Augimeri, A., Cherubini, A., Pantano, P., Zito, G., Lanza, P., Valentino, P., Gioia, M., Quattrone, A.: A cellular neural network methodology for the automated segmentation of multiple sclerosis lesions. J. Neurosci. Methods **203**(1), 193–199 (2012)
7. Chalmers, A., Cohen, A., Bursill, C., Myerscough, M.: Bifurcation and dynamics in a mathematical model of early atherosclerosis: how acute inflammation drives lesion development. J. Math. Biol. **71**(6–7), 1451–1480 (2015)
8. Dolak, Y., Schmeiser, C.: The Keller-Segel model with logistic sensitivity function and small diffusivity. SIAM J. Appl. Math. **66**(1), 286–308 (2006)
9. Gambino, G., Lombardo, M., Sammartino, M.: Turing instability and traveling fronts for a nonlinear reaction-diffusion system with cross-diffusion. Math. Comp. Simul. **82**(6), 1112–1132 (2012)
10. Gambino, G., Lombardo, M., Sammartino, M., Sciacca, V.: Turing pattern formation in the Brusselator system with nonlinear diffusion. Phys. Rev. Stat. Nonlinear Soft Matter Phys. 88(4), 042925 (2013)
11. Han, Y., Li, Z., Zhang, S., Ma, M.: Wavefront invasion for a volume-filling chemotaxis model with logistic growth. Comp. Math. Appl. (2016)
12. Hillen, T., Painter, K.: Global existence for a parabolic chemotaxis model with prevention of over-crowding. Adv. Appl. Math. **26**(4), 280–301 (2001)
13. Hillen, T., Painter, K.J.: A user's guide to PDE models for chemotaxis. J. Math. Biol. **58**(1–2), 183–217 (2009)
14. Keller, E., Segel, L.: Model for chemotaxis. J. Theor. Biol. **30**(2), 225–234 (1971)
15. Khonsari, R., Calvez, V.: The origins of concentric demyelination: Self-organization in the human brain. PLoS One **2**(1), e150 (2007)
16. Lassmann, H.: Multiple sclerosis pathology: evolution of pathogenetic concepts. Brain Pathol. **15**(3), 217–222 (2005)
17. Luca, M., Chavez-Ross, A., Edelstein-Keshet, L., Mogilner, A.: Chemotactic signaling, microglia, and Alzheimer's disease senile plaques: is there a connection? Bull. Math. Biol. **65**(4), 693–730 (2003)

18. Lucchinetti, C., Brück, W., Parisi, J., Scheithauer, B., Rodriguez, M., Lassmann, H.: Heterogeneity of multiple sclerosis lesions: implications for the pathogenesis of demyelination. Ann. Neurol. **47**(6), 707–717 (2000)
19. Mulone, G., Rionero, S., Wang, W.: The effect of density-dependent dispersal on the stability of populations. Nonlinear Anal. Theory Methods Appl. **74**(14), 4831–4846 (2011)
20. Mulone, G., Straughan, B.: Nonlinear stability for diffusion models in biology. SIAM J. Appl. Math. **69**(6), 1739–1758 (2009)
21. Penner, K., Ermentrout, B., Swigon, D.: Pattern formation in a model of acute inflammation. SIAM J. Appl. Dyn. Syst. **11**(2), 629–660 (2012)
22. Quinlan, R., Straughan, B.: Decay bounds in a model for aggregation of microglia: application to Alzheimer's disease senile plaques. Proc. Royal Soc. A Math. Phys. Eng. Sci. **461**(2061), 2887–2897 (2005)
23. Rionero, S.: Multicomponent diffusive-convective fluid motions in porous layers: ultimately boundedness, absence of subcritical instabilities, and global nonlinear stability for any number of salts. Phys Fluids **25**(5), 054104 (2013)
24. Rionero, S.: Soret effects on the onset of convection in rotating porous layers via the "auxiliary system method". Ricerche di Matematica **62**(2), 183–208 (2013)
25. Rionero, S.: L^2-energy decay of convective nonlinear pdes reactiondiffusion systems via auxiliary odes systems. Ricerche di Matematica **64**(2), 251–287 (2015)
26. Rionero, S., Vitiello, M.: Stability and absorbing set of parabolic chemotaxis model of escherichia coli. Nonlinear Anal. Model. Control **18**(2), 210–226 (2013)
27. Sherratt, J.: Wavefront propagation in a competition equation with a new motility term modelling contact inhibition between cell populations. Proc. Royal Soc. A Math. Phys. Eng. Sci. **456**(2002), 2365–2386 (2000)
28. Wrzosek, D.: Global attractor for a chemotaxis model with prevention of overcrowding. Nonlinear Anal. Theory Methods Appl. **59**(8), 1293–1310 (2004)